Available online at www.sciencedirect.com
ScienceDirect
Trans. Nonferrous Met. Soc. China 20(2010) 1305−1310
Transactions of Nonferrous Metals Society of China
www.tnmsc.cn

Influence of impurities on damping properties of ZK60 magnesium alloy

CHEN Xian-hua(陈先华)[1, 2], MAO Jian-jun(毛建军)[1], PAN Fu-sheng(潘复生)[2],
PENG Jian(彭 建)[1, 2], WANG Jing-feng(王敬丰)[1, 2]

1. College of Materials Science and Engineering, Chongqing University, Chongqing 400044, China;
2. National Engineering Research Center for Magnesium Alloys, Chongqing University, Chongqing 400044, China

Received 23 September 2009; accepted 30 January 2010

Abstract: The influence of impurities on damping capacities of ZK60 magnesium alloys in the as-cast, as-extruded and T4-treated states was investigated by dynamically mechanical analyzer at room temperature. Granato and Lucke dislocation pinning model was employed to explain damping properties of the alloys. It is found that reducing impurity content can decrease the amount of second-phase particles, increase grain size and improve damping capacity of the as-cast alloy slightly. The as-extruded alloy with lower impurity content is found to possess obviously higher damping capacity in the relatively high strain region than that with higher impurity concentration, which appears to originate mainly from different dislocation characteristics. The variation tendency of damping property with change of impurity content after solution-treatment is also similar to that in the as-extruded and as-cast states. Meanwhile, the purification of the alloy results in an evident improvement in tensile yield strength in the as-extruded state.

Key words: ZK60 magnesium alloy; impurities; damping; dislocation

1 Introduction

With the development in the modern industry and transportation, noise pollution has become one of major environmental problems. The development and application of high damping materials is one of the effective measures to reduce vibration and noise. Pure magnesium possesses extraordinary high damping capacity, low density and good machinability[1−2]. However, the poor mechanical properties of pure magnesium (e.g. the tensile strength of only about 100 MPa and the elastic modulus of about 40 GPa[3]) restrict its practical engineering application. In the vast majority of cases, the mechanical properties can be improved by alloying, while the damping capacity diminishes evidently[4−7]. Until now, experimental results have shown that neither heat treatment and plastic deformation nor addition of elements could efficiently enhance the damping capacity of magnesium alloys[6, 8]. Hence, it is urgent for researchers to resolve the contradiction between damping capacity and mechanical properties, and to develop magnesium-based damping alloys with high damping and sufficient mechanical properties.

The damping behavior of magnesium and its alloys is considered to be mainly caused by the movement of dislocations which is impeded by impurity atoms, precipitates, grain boundaries and nodes of dislocation network on the basal planes[9]. The interaction between moving dislocations and point defects is one of the major internal friction mechanisms of magnesium and its alloys[10]; consequently, the impurities may have a significant effect on damping characteristics. RIEHEMANN and ABED EL-AL[11] demonstrated that damping value in high-purity magnesium was generally higher than in commercial-purity magnesium at room temperature. Whereas, there has been almost no systematical study on the relation between internal friction and impurity elements for magnesium alloys until now.

The present work aims to examine the effect of impurity content on damping capacities and tensile properties of ZK60 alloys in various states, since this alloy is one of the most typical high-strength wrought magnesium alloys. Based on microstructural observations, the dislocation damping mechanism is also discussed.

Foundation item: Project(50725413) supported by the National Natural Science Foundation of China; Project(2009BB4215) supported by the Natural Science Foundation of Chongqing Science and Technology Commission, China; Project (2008AB4114) supported by the Major Program of Chongqing Science and Technology Commission, China
Corresponding author: CHEN Xian-hua; Tel: +86-15922784658; E-mail: xhchen@cqu.edu.cn
DOI: 10.1016/S1003-6326(09)60295-8

2 Experimental

The materials used in the present experiments were high-strength ZK60 magnesium alloys. The alloy ingots of ZK60 were prepared from high-purity Mg (99.98%), pure Zn (99.9%) and Mg-27.85%Zr (mass fraction) master alloys in an electric resistance furnace under the flux protection. When the temperature reached 780 ℃, the molten alloy was stirred for 8 min and subsequently held for 30 min and 45 min, respectively. Then, the molten alloy was poured into steel molds and cast into two cylindrical ingots with 1.5 m in height and 90 mm in diameter. The actual chemical compositions of the alloys were determined by a photoelectricity spectrum analyzer (APL4460). The two as-cast ingots were machined into cylinder-shaped ingots with a diameter of 85 mm for extrusion. The ingots were homogenized at 420 ˚C for 18 h and then extruded into rods with diameter of 16 mm at 390 ˚C, which generated an extrusion ratio of 27:1. Solid solution treatment (T4, at 450 ˚C for 5 h, cooled in air) was finally performed for the as-extruded alloys.

The damping capacities of ZK60 alloys were measured using a dynamic mechanical analyzer (DMA, Model TA Q800) with single cantilever vibration mode at room temperature. The dimension of the damping test specimen was 45 mm×5 mm×1 mm. One end of the specimen was properly installed in a fixed clamp and the other end was installed in a movable clamp. The damping value was determined by Q^{-1}=tan Φ, where Φ was the lag angle between the applied strain and the response strain. Measurements were made in the strain amplitude range from 1×10^{-5} to 5×10^{-3} and the vibration frequency was 1 Hz. Tensile specimens with a gauge length of 50 mm and a diameter of 5 mm were machined along the extrusion direction. Tensile tests were performed on a mechanical testing machine (CMT-5105) with a constant strain rate of 1×10^{-3} s^{-1} at room temperature. Optical microscopy (OM) and scanning electron microscopy (SEM, TESCAN VEGA Ⅱ LMU) were employed to analyze the microstructures of ZK60 alloys. All the specimens for OM and SEM observations were etched with picric acid.

3 Results

3.1 Impurity analysis

The chemical compositions of the two alloys are listed in Table 1. In Table 1, ZK60 ingot with holding time of 30 min is hereafter referred to as ZK60-30, and the ingot with holding time of 45 min is referred to as ZK60-45. The total content of the impurities in ZK60-45 is approximately 0.007 3% (mass fraction), which is lower than the value of 0.010 1% (mass fraction) in ZK60-30. In molten metal, Zr and several impurity elements (Fe, Si, Mn, etc) could form insoluble stable compounds with high melting point[12−13]. Therefore, increasing holding time facilitates such phenomenon that these compounds settle to the bottom of the crucible, which causes a decrease of impurity content in cast ingots.

Table 1 Chemical compositions of alloys (mass fraction, %)

Alloy	Si	Fe	Cu	Mn	Be
ZK60-30	0.003 2	0.002 0	0.000 61	0.003 9	0.000 34
ZK60-45	0.002 0	0.001 3	0.000 45	0.003 4	0.000 11

Alloy	Ni	Zn	Zr	Mg
ZK60-30	<0.000 5	6.37	0.53	Bal.
ZK60-45	<0.000 5	6.21	0.53	Bal.

3.2 Microstructure

The typical optical microstructures of two ZK60 alloys with various impurity contents in different states are shown in Fig.1. Obviously, both ZK60 samples in the as-cast state have a microstructure consisting of primary Mg matrix and black semi-continuous eutectic constituents distributed at the grain boundaries (as shown in Figs.1(a) and (b). According to XRD and DSC analysis, the eutectic phase formed at about 340 ˚C could be described as MgZn. Some black particles precipitated around the grain boundaries and within the grains may be $MgZn_2$. It is evident that the black particles are more in the as-cast ZK60-30 as compared with those in the as-cast ZK60-45. The average grain sizes are measured to be 125 μm and 151 μm for ZK60-30 and ZK60-45, respectively.

The transverse microstructures of the two ZK60 samples after extrusion at 390 ℃ are illustrated in Figs.1(c) and (d). It is found that significant dynamic recrystallization (DRX) has occurred in both samples, which results in a considerable grain refinement. Observations show that the recrystallized grains are mostly equiaxed with well-defined grain boundaries. Some second phase particles precipitated inside the matrix grains are observed. Whereas, the structure is somewhat inhomogeneous, and the DRX grains have two populations of grain sizes due to the incomplete dynamic recrystallization in some regions. The coarse grains are 50−100 μm in size while the fine grains are 5−20 μm. The average size of the as-extruded ZK60-30 is seen to be larger than that of the as-extruded ZK60-45. The difference in grain size between two magnesium alloys seems to be related with the effect of impurity elements on DRX.

As shown in Figs.1(e) and (f), compared with the sample in as-extruded state, the tendency of grain growth

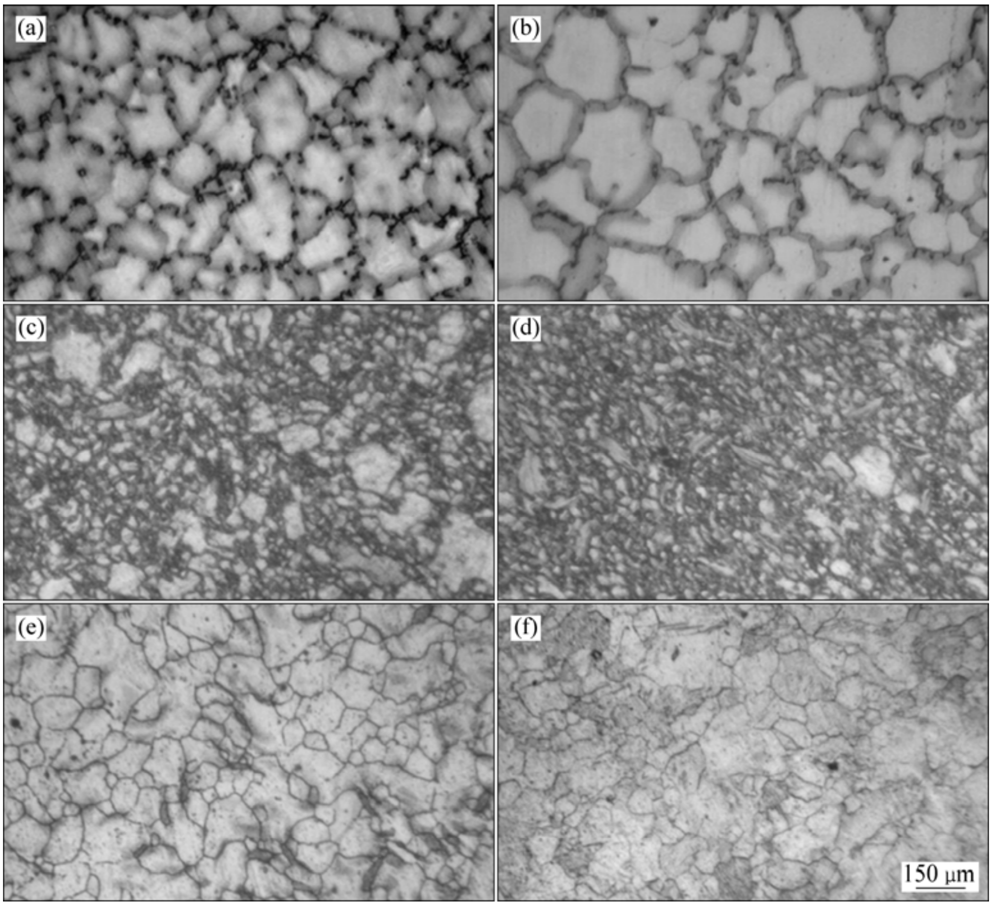

Fig.1 Typical optical micrographs of two ZK60 alloys with various impurity contents in different states: (a) As-cast ZK60-30; (b) As-cast ZK60-45; (c) As-extruded ZK60-30; (d) As-extruded ZK60-45; (e) T4-treated ZK60-30; (f) T4-treated ZK60-45

is very obvious in both alloys after solid solution treatment at 420 ℃ for 8 h. Moreover, the grain boundary width reduces to a certain extent, which originates from the dissolving of second phase constituent at high temperature. It can be found that the grain size of ZK60-45 is still larger as compared with ZK60-30.

3.3 Damping properties

The strain dependence of damping capacity of ZK60-30 and ZK60-45 alloys in the as-cast, as-extruded and T4-treated states are shown in Fig.2. All the damping curves have the similar characteristic that the damping capacity can be divided into two parts[9]:

$$Q^{-1}(\varepsilon)=Q_0^{-1}+Q_{\mathrm{H}}^{-1}(\varepsilon) \tag{1}$$

where Q_0^{-1} and Q_{H}^{-1} represent the strain-independent damping and strain-dependent damping, respectively. At lower strain amplitude region (ε<5×10^{-4}), the strain-independent damping value keeps constant, which corresponds to the level part of damping curves. With strain amplitude beyond the critical strain amplitude (ε_c, the turn point between the strain-independent damping and the strain-dependent damping), the damping values rise rapidly with strain amplitude increasing. It is clear from Fig.2 that for all of ZK60 alloys, the as-cast specimen shows the highest internal friction value, while the as-extruded specimen exhibits the lowest value when the strain is above ε_c. As for the T4-treated specimen, its internal friction value is between the value of the as-cast and the as-extruded specimens.

Fig.2 indicates that Q_{H}^{-1} values are improved and Q_0^{-1} values do not almost show any obvious variation by reducing impurity elements for the ZK60 specimens whether in the as-cast, as-extruded, or T4-treated states. At strain of 1×10^{-3}, the damping capacity is increased by 17%, 38% and 19%, respectively. In contrast to the strain-dependent damping, ε_c becomes lower with reducing impurities in the alloys, as seen in Table 2.

3.4 Tensile properties

It is very interesting to investigate the tensile properties of the as-extruded specimens since reducing impurity content causes a great enhancement of damping values in the as-extruded state. The tensile test results of the as-extruded ZK60-30 and ZK60-45 are displayed in Fig.3. It is found that the two specimens have a similar

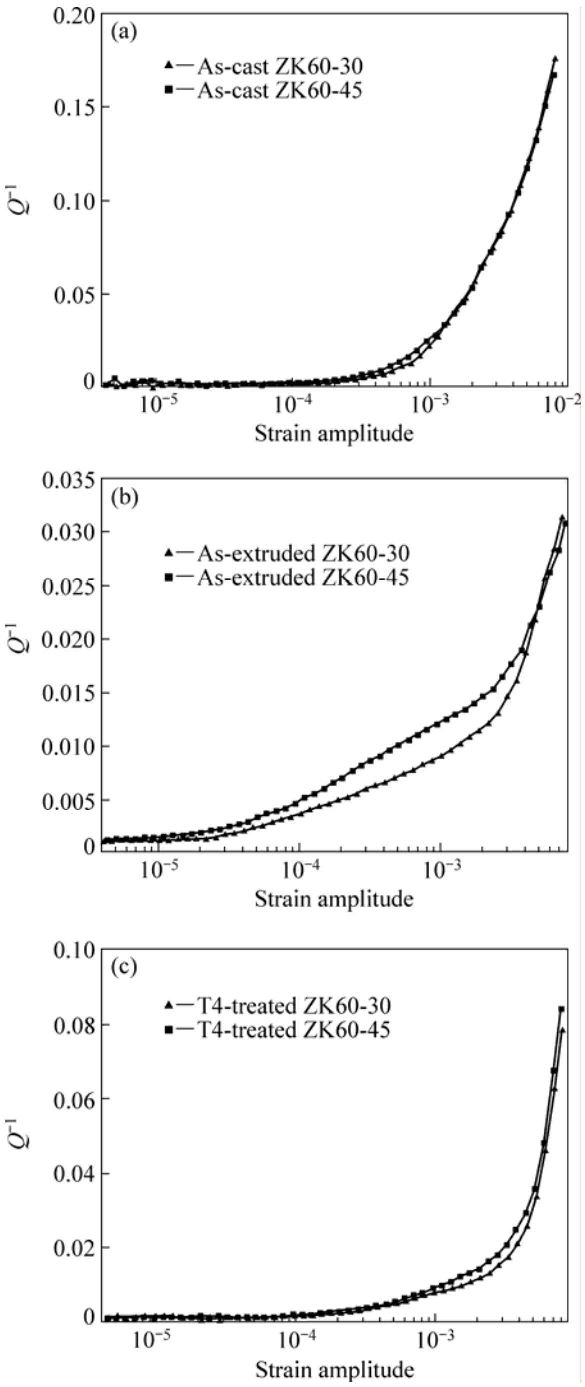

Fig.2 Damping capacities plotted as function of strain amplitude for alloys in as-cast (a), as-extruded (b) and T4-treated (c) states

Table 2 Critical strain amplitude and values of parameters obtained from G-L plot

Alloy	C_1	C_2	ε_c
As-cast ZK60-30	2.04×10^{-4}	0.002 08	1.32×10^{-4}
As-extruded ZK60-30	2.61×10^{-5}	1.02×10^{-3}	2.21×10^{-5}
T4-treated ZK60-30	2.10×10^{-4}	0.004 08	5.25×10^{-5}
As-cast ZK60-45	2.67×10^{-4}	0.001 76	9.37×10^{-5}
As-extruded ZK60-45	3.30×10^{-5}	9.75×10^{-4}	1.21×10^{-5}
T4-treated ZK60-45	2.42×10^{-4}	0.003 95	6.01×10^{-5}

elongation-to-failure of about 19.1%, while they possess different ultimate tensile strength (σ_b) and yield strength (σ_s) values. When the whole impurity content decreases from 0.010 1% to 0.007 3%, the σ_s exhibits an increase of 24.3 MPa, higher than that for σ_b (6.9 MPa). This also suggests that higher work hardening has occurred in the ZK60-30 sample with more impurity elements.

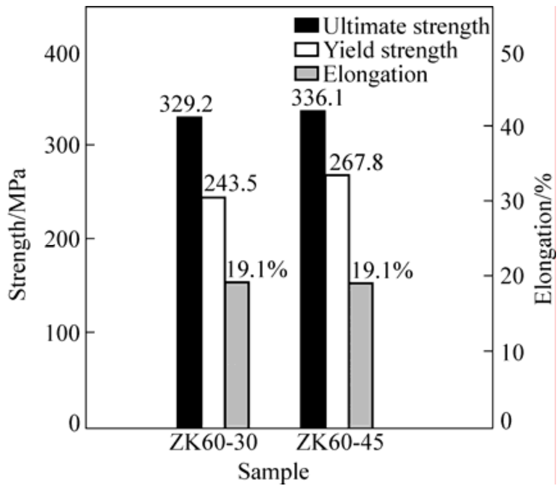

Fig.3 Tensile properties of as-extruded alloys

4 Discussion

The influence of purification on damping capacity is taken into account. Various factors contributing to damping capacities of materials include crystalline defects, dislocation motion, grain boundary sliding and magnetoelastic effects. In magnesium and its alloys, the damping response is dominantly due to the dislocation mechanism. Consequently, the above mentioned experimental results can be interpreted by the dislocation string model of Granato and Lücke (G-L).

According to the model, in case of small oscillating stress, dislocation segments only bow out between weak pinning points with mean distance L_d (Fig.4), leading to strain-independent damping Q_0^{-1}. The value of Q_0^{-1} can be expressed as

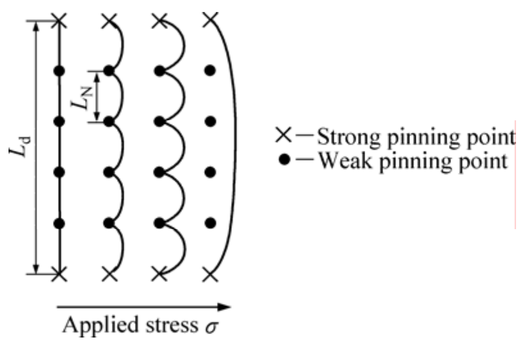

Fig.4 Dislocation string model of Granato and Luicke[9] illustrating bowing out and breakaway by increasing applied stress

$$Q_0^{-1}=\rho L_{\rm d}^4 \tag{2}$$

where ρ is the dislocation density. When the applied stress is large enough, the dislocation segments are broken away from the weak pinning points but still pinned by strong pinning points. This process produces strain- dependent damping, $Q_{\rm H}^{-1}$, which can be calculated as

$$Q_{\rm H}^{-1}=\frac{C_1}{\varepsilon}\exp\left(-\frac{C_2}{\varepsilon}\right) \tag{3}$$

$$C_1=\frac{\rho F_{\rm B}L_{\rm N}^3}{6bEL_{\rm d}^2},\ C_2=\frac{Kb\eta}{L_{\rm d}} \tag{4}$$

where $F_{\rm B}$ is the binding force between a dislocation and a solute atom (weak pinning point), E is the unrelaxed modulus, ε is the strain amplitude, $L_{\rm N}$ is the mean length of dislocation segments between strong pinning points (Fig.4), b is the magnitude of Burger vector, K is constant and η is the size ratio of solvent to solute atoms. Eq.(3) may be alternated as

$$\ln(Q_{\rm H}\varepsilon)=\ln C_1-\frac{C_2}{\varepsilon} \tag{5}$$

and the G-L plots (i.e. $\ln(Q_{\rm H}^{-1}\varepsilon)$ versus ε^{-1}) should be straight lines, whose intercept and slope are the values of ln C_1 and C_2, respectively.

The results of G-L plots of ZK60 specimens are shown in Fig.5, and the values of C_1 and C_2 are given in Table 2. It is observed that the diminishing of impurity elements enhances C_1 value while reduces C_2 value. This produces a higher $Q_{\rm H}^{-1}$ value for ZK60-45 as compared with ZK60-30 according to Eq.(3), which is consistent with the observed results in Fig.2. To explain it, the changes in movable dislocation density, second phase precipitates (strong pinning point), amounts of impurity atoms (weak pinning point) and nodes of dislocation network (strong pinning point) should be taken into account according to Eq.(4).

As lower amount of impurity atoms increases the values of $L_{\rm d}$, C_2 values are lower in ZK60-45 specimens in the as-cast, as-extruded and T4-treated states. Since the grain size is larger and the quantity of second phase precipitates ($MgZn_2$, MgZn, etc) is smaller in the as-cast ZK60-45 as compared with ZK60-30, $L_{\rm N}$ of the as-cast ZK60-45 should be greater, which is responsible for the increased C_1 value. As seen in Figs.1(c) and (d), more sufficient dynamic recrystallization has occurred in ZK60-45 during hot extrusion, which facilitates to reduce dislocation tangles, resulting in improved movable dislocation density ρ and $L_{\rm N}$ in the as-extruded ZK60-45 although its grain size is smaller than that of the as-extruded ZK60-30. This may generate a larger C_1 value for the as-extruded ZK60-45. Solution treatment has a similar effect on the microstructures of both alloys, so it is rather reasonable that the C_1 values of the T4-treated specimens exhibit the same variation tendency as that of the as-extruded specimens when the purity content increases. Hence, it can be concluded that the difference in strain-dependent damping capacity between ZK60-45 and ZK60-30 should dominantly originate from second phase precipitation in the as-cast state and dislocation characteristics in the as-extruded state.

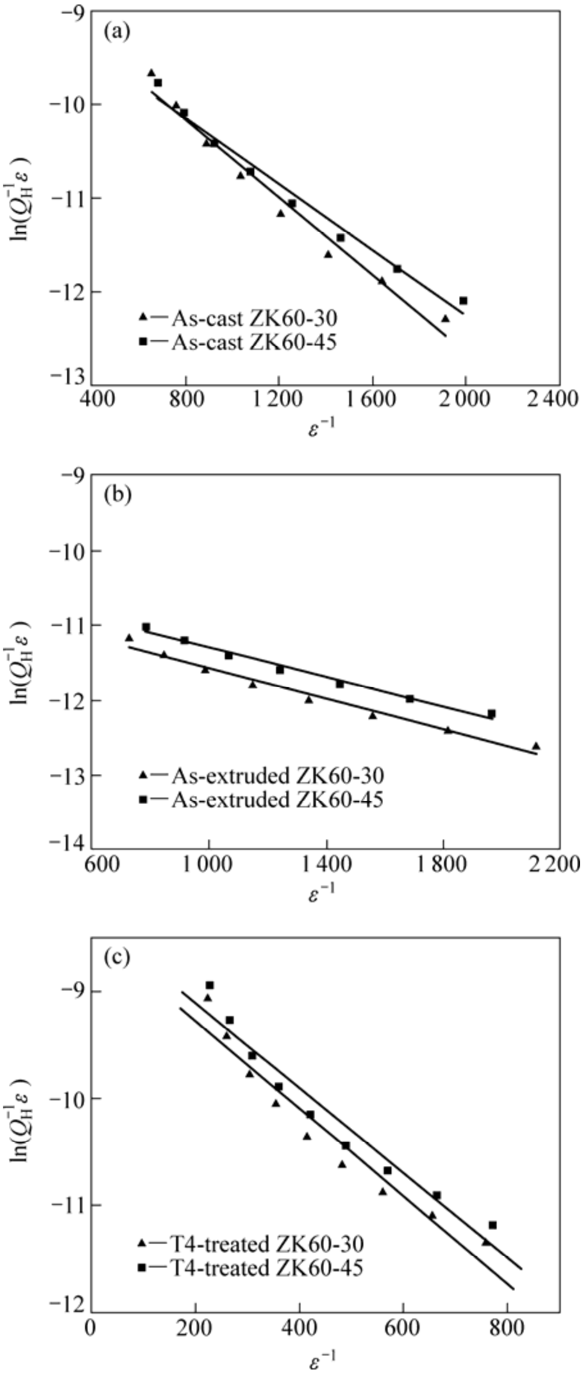

Fig.5 G-L plots of ZK60 alloys in as-cast (a), as-extruded (b) and T4-treated (c) states

For ZK60-45 and ZK60-30, the damping values of the as-cast specimen is considerably higher than those of the as-extruded and T4-treated specimens, which may be mainly attributed to the fact that hot extrusion deformation greatly refines grains of the material, i.e. increases strong pinning points. Most second phase particles in grains are dissolved into the matrix and these grains grow after T4 treatment, as a result, the strain-dependent damping capacity is found to be greater for the T4-treated specimen as compared with the as-extruded one[14−15].

The improvement in tensile strength could be dominantly ascribed to the grain refinement effect in the micrometer scale, in which lattice dislocation motions are blocked by numerous amounts of grain boundaries. On the other hand, impurity elements may influence the slip system activation, causing the variation of yield strength in magnesium alloys, as observed in magnesium by KUTSUKAKE et al[16].

5 Conclusions

1) Impurity content of ZK60 magnesium alloy is decreased by means of increasing holding time of alloy melt properly during semi-continuous casting.

2) In the as-cast, as-extruded and T4-treated states, the reduction of impurity content improves damping capacity of the alloy in relatively high strain region. Wherein, the increment of damping capacity in the as-extruded state is the most obvious. The experimental results can be ascribed to less impurity atom pinning, lower amount of second phase precipitates and improved dislocation characteristics in the alloy.

3) Purification of alloys is found to be very potential to develop high-performance magnesium alloys with optimized combination of damping capacities and mechanical properties.

References

[1] JAMES D W. High damping metals for engineering applications [J]. Materials Science and Engineering, 1969, 4: 1−8.

[2] HU X S, ZHANG Y K, ZHENG M Y, WU K. A study of damping capacities in pure Mg and Mg-Ni alloys [J]. Scripta Materialia, 2005, 52: 1141−1145.

[3] SRIKANTH N, ZHONG X L, GUPTA M. Enhancing damping of pure magnesium using nano-size alumina particulates [J]. Materials Letters, 2005, 59: 3851−3855.

[4] AVEDESIAN M M, BAKER H. ASM specialty handbook [M]. Ohio: ASM International, the Materials Information Society, 1999.

[5] SUGIMOTO K, NIIYA K, OKAMOTO T, KISHITAKE K. A study of damping capacity in magnesium alloys [J]. Transaction of JIM, 1977, 18: 277−280.

[6] WANG Jing-feng, ZHAO Liang, HU Yao-bo, PENG Jian, ZHANG Ding-fei, PAN Fu-sheng, DING Pei-dao. Research status and prospect of damping magnesium alloys [J]. Materials Review, 2008, 22(7): 103−106. (in Chinese)

[7] GOKEN J, SWIOSTEK J, LETZIG D, KAINER K U. Damping measurements of the magnesium wrought alloys AZ31, AZ61 and AZ80 after indirect and hydrostatic extrusion [J]. Materials Science Forum, 2005, 482: 387−390.

[8] HU X S, WU K, ZHENG M Y, GAN W M, WANG X J. Low frequency damping capacities and mechanical properties of Mg-Si alloys [J]. Materials Science and Engineering A, 2007, 452/453: 374−379.

[9] GRANATO A, LUCKE K. Theory of mechanical damping due to dislocations [J]. Journal of Applied Physics, 1956, 27(6): 583−593, 789−805.

[10] LIAO Li-hua, ZHANG Xiu-qin, LI Xian-feng, WANG Hao-wei, MA Nai-heng. Effect of silicon on damping capacities of pure magnesium and magnesium alloys [J]. Materials Letters, 2007, 61: 231−234.

[11] RIEHEMANN W, ABED EL-AL F. Influence of ageing on the internal friction of magnesium [J]. Journal of Alloys and Compounds, 2000, 310: 127−130.

[12] WU Guo-hua, GAO Hong-tao, DING Wen-jiang, ZHU Yan-ping. Study on mechanism of iron reduction in magnesium alloy melt [J]. Journal of Materials Science, 2005, 40: 6175−6180.

[13] WAN Peng, FAN Xiao-ming, HU Shou-yu, WEN Hong-yan. Harmful effect of Fe on properties of magnesium alloy and neutralizing methods [J]. Research Studies on Foundry Equipment, 2008, 1(1): 11−14. (in Chinese)

[14] ZHANG Zhen-yan, ZENG Xiao-qin, DING Wen-jiang. The influence of heat treatment on damping response of AZ91D magnesium alloy [J]. Materials Science and Engineering A, 2005, 392: 150−155.

[15] WAN Di-qing, WANG Jin-cheng, WANG Gai-fang, LIN Lin, FENG Zhi-gang, YANG Gen-cang. Precipitation and responding damping behavior of heat-treated AZ31 magnesium alloy [J]. Acta Metallurgica Sinica (English Letters), 2009, 22(1): 1−6.

[16] KUTSUKAKE A, ANDO S, TSUSHIDA M, KITAHARA H, TONDA H. Influence of impurities to deformation behavior in magnesium single crystal [J]. Key Engineering Materials, 2007, 345/346: 137−140.

(Edited by YANG Bing)